Critical Angles for Channeling of 1- to 25-keV H^+, D^+, and He^+ Ions in Gold Crystals*

C. J. ANDREEN† AND R. L. HINES
Northwestern University, Evanston, Illinois
(Received 6 February 1967)

The critical angle for channeling in the low-energy region is measured for H^+, D^+, and He^+ ions transmitted through single-crystal gold foils. It is found that the theoretical calculation by Lindhard fits the experimental points within the experimental errors if the constant C is given the value 2.15. No difference is found between H^+ and D^+ ions. The critical angle for He^+ ions is found to be 1.13 ± 0.04 times larger than for D^+ or H^+ ions of the same energy.

IT has been shown by Nelson and Thompson that it is possible to detect surprisingly high intensities of H^+ ions transmitted through thick (3000–4000 Å) single-crystal gold films in the ⟨110⟩ directions at an ion energy of 75 keV.[1] The presence of the channeled ions showed up as peaks in the ion intensity measured as a function of crystal orientation with respect to the incident beam direction. Peaks due to the channeled ions were seen for both transmitted and reflected ions. However, no energy analysis was made of the ions and no detailed comments were made concerning the angular widths of the peaks. Recently we have reported preliminary results on the angular widths of the peaks at low energies.[2] At higher energies (15–25 keV) a detailed investigation has shown the geometrical relationships between the angular widths of the peaks measured under different conditions.[3]

A recent analysis of the influence of a crystal lattice on the motion of energetic charged particles by Lindhard[4] shows that one can expect to find certain specific characteristics in the transmission curve. One such characteristic is a critical angle for channeling. This critical angle can be related to the half-width of the experimentally observed peak. The critical angle is derived for both a high-energy and a low-energy region. The analysis is primarily concerned with high energies, but an approximate expression is given for the low-energy region.

This paper gives experimental results for the angular widths of the channeled peaks for 1- to 25-keV H^+, D^+, and He^+ ions in gold crystals and compares these results with the theoretical predictions of Linhard in the low-energy region.

THEORY

The approximate expression derived by Lindhard[4] for the critical angle ψ for channeling is based on the continuum string approximation. It is demanded that the scattering at the point of closest approach to a nucleus along the path should be due to several atoms. At reasonable distances from the nucleus the average potential of many atoms lined up in a row (as, for example, along a low-index crystallographic direction in a single crystal) is described by the so-called string potential. This transverse potential $U(r)$, where r is the distance from the string, is an average of potentials $V(R)$ of the Thomas–Fermi type,

$$V(R)=Z_1Z_2e^2R^{-1}\varphi_0(R/a). \tag{1}$$

R is the ion-atom distance, Z_1 is the atomic number of the incident particle, Z_2 is the atomic number of the stopping medium, $a=0.885a_0(Z_1^{2/3}+Z_2^{2/3})^{-1/2}$, and $\varphi_0(R/a)$ is the Fermi function belonging to one isolated atom. $U(r)$ is then given by

$$U(r)=Z_1Z_2e^2d^{-1}\xi(r/a), \tag{2}$$

where d is the distance between atoms along the string. An approximate expression for $\xi(r/a)$ which is applicable for all values of r is given by

$$\xi(r/a)=\ln[(Ca/r)^2+1]. \tag{3}$$

The adjustable constant C may be given the value $C=\sqrt{3}$ to give a good over-all fit, but it will be slightly higher for large values of r/a.

The condition that the scattering in the vicinity of the minimum distance approach, $r_{\min}$, is due to many atoms leads to the relation

$$r_{\min}>d\psi, \tag{4}$$

where ψ is the critical angle for channeling. The minimum distance of approach is determined by

$$U(r_{\min})=\tfrac{1}{2}M_1v^2\sin^2\psi, \tag{5}$$

where M_1 is the mass of the incident particle and v its velocity. From Eqs. (2), (3), (4), and (5) it can be shown that the critical angle ψ_1 for channeling in the high-energy region is given by

$$\psi_1=(2Z_1Z_2e^2/dE)^{1/2}, \tag{6}$$

where E is the energy of the incident ion. Equation (6) is valid as long as $Ca/\psi_1 d$ is larger than unity, which is approximately equivalent to the condition

$$E>E'=2Z_1Z_2e^2d/a^2. \tag{7}$$

* Supported by the U. S. Atomic Energy Commission.
† Present address: Chalmers University of Technology, Gothenburg, Sweden.
[1] R. S. Nelson and N. W. Thompson, Phil. Mag. **8**, 1677 (1963).
[2] C. J. Andreen and R. L. Hines, Phys. Letters **24A**, 118 (1967).
[3] C. J. Andreen and R. L. Hines, Phys. Rev. **151**, 341 (1966).
[4] J. Lindhard, Kgl. Danske Videnskab. Selskab. Mat. Fys. Medd. **34**, No. 14 (1965).

At low energies, where $E<E'$, the quantity $Ca/\psi_1 d$ is small compared to unity, yielding

$$\psi_2=(C^2a^2Z_1Z_2e^2/Ed^3_{hkl})^{1/4}, \quad (8)$$

where ψ_2 is the critical angle for channeling in the low-energy region and d is given the subscript hkl to denote a particular direction. This equation for ψ_2 is a rough estimate and can hardly be expected to hold at very low energies.

A classical treatment for the motion of the particles is appropriate here. The stopping is almost exclusively due to electronic stopping. The nuclear stopping is only 1% of the electronic stopping in this energy region for a random system.[5] The nuclear stopping is further reduced when the particles are moving along an open direction in the crystal. At low velocities ($v<v_0$) the electronic energy loss can be approximately calculated from the equation

$$(dE/dx)_e=8\pi Ne^2a_0Z_1Z_2\xi_e(Z_1^{2/3}+Z_2^{2/3})^{-3/2}v/v_0 \quad (9)$$

given by Lindhard and Scharff,[5] where v is the incident particle velocity, $v_0=e^2/\hbar$, and $\xi_e\simeq Z_1^{1/6}$.

EXPERIMENTAL APPARATUS AND PROCEDURE

The bombarding equipment and the goniometer and detector geometry have been described elsewhere.[3,6] The important parameter which is varied in this experiment is the energy of the incident particle. The lowest incident-ion energy is set by the thickness of the gold foil and the sensitivity of the detection system. The upper energy limit is set by voltage isolation conditions in the equipment. Because of radiation damage and contamination build up, the time available for bombardment without introducing large errors is shorter at the higher energies. A practical energy interval for the present equipment is found to be about 1 to 25 keV. The measuring procedure has been described in detail earlier.[3] The only difference in this experiment is that the bombarding times and thus the total amounts of radiation damage are kept small by concentrating the measurements on the peaks and their immediate surroundings. Measurements for all orientations of the foil are taken for only a few of the foils.

The gold films are made by vacuum evaporation of gold onto silver which in turn has been vacuum evaporated onto rocksalt. After the gold films have been stripped from the rocksalt and silver they are mounted on 75-mesh grids. The details of the growing technique can be found elsewhere.[7] The mounted foils are examined for wrinkles using an optical microscope and foils with any visible wrinkles are discarded. The foils are also examined with an electron microscope. The thicknesses of the foils are checked by measuring the projections of the stacking faults on the plane of observation. The foils usually show bend extinction contours which indicate the presence of submicroscopic wrinkles. The amount of the variation in foil orientation is checked by observing the selected area diffraction patterns from small areas. The diffraction pattern for a perfectly flat, thin, single-crystal foil shows Laue zones where the diffraction spots are strong.[8] If the foil is normal to the electron beam, the circular Laue zones are centered on the incident-beam spot. If, however, the film is not normal to the electron beam because of the submicroscopic wrinkles, then the center of the zeroth Laue zone is displaced from the incident-beam spot, the the displacement gives the relative local orientation of the foil. With reasonable care it is possible to set the selected-area mask to a small enough opening so that the variations in orientation within the selected area do not obscure the Laue-zone structure. It is then easy to check the orientation at different points by moving the sample. A typical good foil has a standard deviation in orientation angle of $0.5°\pm0.25°$. According to an earlier estimate of the influence of the foil misorientation on the angular resolution of a channel peak, the effect of the submicroscope wrinkles is found to be less than 1%.

RESULTS AND DISCUSSION

Figure 1(a) shows the energy spectrum for 12-keV D^+ ions channeled along the [011] direction in a 350–400 Å thick gold foil. The final particle energy E_f in keV is determined from the voltage U in kilovolts applied to the plates of the electrostatic analyzer. In this case

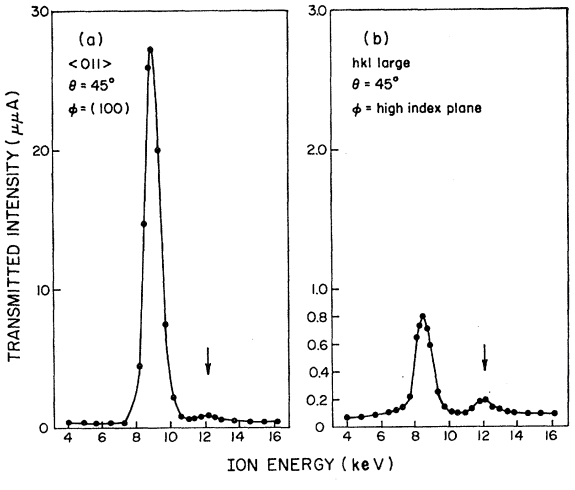

FIG. 1. The transmitted D^+ intensity in the forward direction through a gold foil is shown as a function of the emerging ion energy as determined with an electrostatic analyzer. (a) The foil is oriented in the ⟨011⟩ direction. The arrow indicates the energy of the direct beam. (b) The foil used in (a) is now oriented in a high-index direction with the same tilt angle θ as in (a). The arrow again indicates the energy of the direct beam.

[5] J. Lindhard and M. Scharff, Phys. Rev. **124**, 128 (1961).
[6] R. L. Hines and R. Arndt, Phys. Rev. **119**, 623 (1960).
[7] D. W. Pashley, Phil. Mag. **4**, 324 (1959).
[8] P. B. Hirsch, A. Howie, R. B. Nicholson, D. W. Pashley, and M. J. Whelan, *Electron Microscopy of Thin Crystals* (Butterworths Scientific Publications, Ltd., London, 1965), p. 112.

TABLE I. The most probable relative energy loss $\Delta E_{mp}^{\langle hkl\rangle}/E$ in the directions $\langle 011\rangle$ and $\langle 001\rangle$ and the transmission coefficient T in the forward direction along the $\langle 001\rangle$ channel are given for H^+, D^+, and He^+ ions at a few different values of the incident energy E. The relative energy loss is larger in the $\langle 011\rangle$ direction due to the fact that the effective foil thickness is $\sqrt{2}$ times larger than in the $\langle 001\rangle$ direction.

Foil	Thickness (Å)	Ion	E (keV)	$\Delta E_{mp}^{\langle 011\rangle}/E$	$\Delta E^{\langle 001\rangle}{}_{mp}/E$	$T_{\langle 001\rangle}$
852*NK*	265	H^+	14.3	0.293	0.217	0.02
		D^+	14.3	0.217	0.166	0.04
		He^+	14.9		0.210	0.001
		He^+	28.8		0.154	0.02
853*NK*	250	H^+	14.2	0.270	0.207	0.03
		H^+	28.3	0.189	0.145	0.13
		D^+	14.3	0.192	0.143	0.06
		D^+	28.5	0.137	0.100	0.15
		He^+	14.8		0.170	0.002
854*NK*	260	H^+	14.2	0.298	0.237	0.02
		H^+	28.4	0.212	0.168	0.10
		D^+	14.1	0.244	0.183	0.05
		D^+	28.4	0.174	0.136	0.13
		He^+	14.9	0.303	0.220	0.0003

$E_f = 8.13\,U$. This relationship is found from energy analysis of the incident beam with the foil removed and agrees with the value calculated from the geometry of the analyzer. Figure 1(b) shows the energy spectrum for an azimuthal angle of rotation φ around the foil normal such that the ions travel along a high-index direction in the crystal. One observes that the intense peak decreases by a factor of about 40 when φ is changed from a low-index direction [Fig. 1(a)] to a high-index direction [Fig. 1(b)]. The small peaks in both figures indicate the energy of the direct beam. In this particular run the intensity of the direct peak relative to the channel peak is extraordinarily high and is probably due to a small tear in the foil. Normally nothing is seen at all of the direct beam. The most probably energy loss $\Delta E_{mp}^{(r)}$, as determined from Fig. 1(b) for *hkl* large, is given the superscript (r) to indicate that the direction has a high index. The difference $\Delta E_{mp}^{\langle 011\rangle} - \Delta E_{mp}^{(r)}$ is due to the effect of channeling on the energy loss. The results of the energy-loss measurements are summarized in Table I. The transmission T, which is the ratio of the transmitted intensity in the forward direction to the incident intensity, is also given in Table I. It is a function of the foil perfection and flatness and is included here to give an idea of its magnitude.

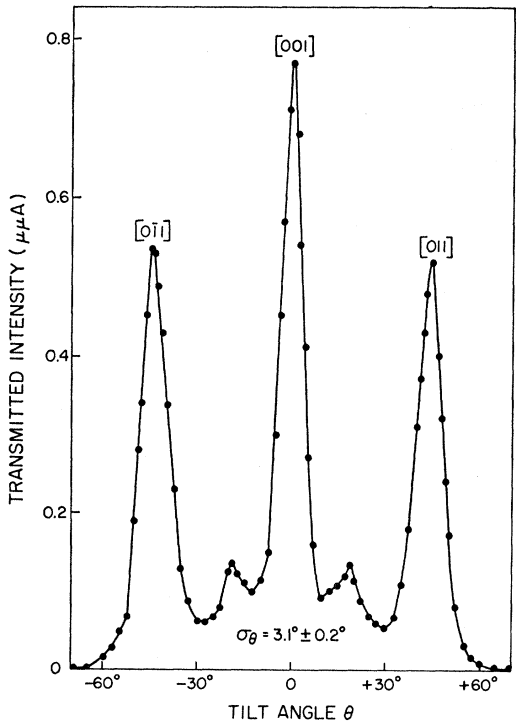

FIG. 2. The transmitted intensity is shown for D^+ ions in the (100) plane as a function of the tilt angle θ. The incident ion energy is 1.8 keV, the incident current is 100 $\mu\mu$A and the foil thickness is about 225Å. The characteristic half-width is found to be $\sigma_\theta = 3.1° \pm 0.2°$ for the $\langle 001\rangle$ peak.

Figure 2 shows the transmitted intensity as a function of tilt angle for D^+ ions of 1.8 keV incident on a 225 Å thick gold single crystal. Figure 3(a) shows the angular distribution in the transmitted intensity when the detector angle α with respect to the incident-beam direction is varied with the foil fixed in the $\langle 001\rangle$ direction. Figure 3(b) shows the distribution for a variation of both θ, the tilt angle, and α such that $\theta = \alpha$, which means that the detector is kept fixed along the $\langle 001\rangle$ direction. In this particular case we obtain for the channel-entrance characteristic half width a value $\sigma_{1\theta} = 4.5° \pm 0.2°$. For the channel-exit characteristic half-width we obtain the value $\sigma_{2\theta} = 4.3° \pm 0.2°$. From Fig. 2 we obtain a value $\sigma_\theta = 3.2° \pm 0.2°$ by changing θ. This value agrees very well with the value 3.1° calculated from simple geometrical considerations.[3] From several measurements of this kind we obtain the relationship

$$\sigma_{1\theta} = (1.0 \pm 0.1)\,\sigma_{2\theta}. \qquad (10)$$

TABLE II. The characteristic half widths σ_θ for transmitted H^+, D^+, and He^+ ions, respectively, are given for the three crystallographic directions ⟨011⟩, ⟨001⟩, and ⟨112⟩ for five different single-crystal gold foils. The probable errors of the numbers are between 5 and 10%.

Foil	E (keV)	H^+ ⟨011⟩	H^+ ⟨001⟩	H^+ ⟨112⟩	D^+ ⟨011⟩	D^+ ⟨001⟩	D^+ ⟨112⟩	He^+ ⟨011⟩	He^+ ⟨001⟩	He^+ ⟨112⟩
823*MN*	23	2.2	2.1	1.9	2.3	2.1	2.0			
837*NH*	3	4.0	3.5	3.0	4.0	3.5	3.0			
883*NR*	18				2.1	1.9	1.6	2.5	2.4	1.9
885*NS*	17				2.6	2.5	2.1	2.8	2.7	2.1
893*TN*	18				2.2	2.1	1.6	2.4	2.3	1.9

A previous estimate[3] of the ratio $\sigma_{1\theta}/\sigma_{2\theta}$ gave the value 0.7 for 25 keV D^+ ions in gold. The suggestion was made that due to the energy loss the value of $\sigma_{2\theta}$ should be slightly higher than $\sigma_{1\theta}$. The ratio is checked here at 1.8, 3.3, and 11.3 keV and is found to be 1.0 ± 0.1. It is true that the energy loss due to electronic excitations and ionizations becomes less important as the energy $\bar{E}$ decreases. Consequently, the focusing effect due to correlated nuclear collisions, which is the origin of the channeling effect, may play a larger role at very low energies and thus make the ratio $\sigma_{1\theta}/\sigma_{2\theta}$ less dependent on energy. Figure 4 shows the pronounced change in angular resolution when the incident D^+ ion energy is increased to 8.5 keV. The same foil is used to obtain the data shown in Figs. 2, 3, and 4.

In order to obtain the critical angle for channeling α_c, the following construction is performed. At the point defining σ, a tangent is drawn towards the background intensity. The angle where the tangent meets this intensity is defined as the experimental critical angle α_c. We find that

$$\alpha_c=(2.14\pm0.18)\sigma_{1\theta}. \tag{11}$$

From (10) and elsewhere[3] we thus find that $\sigma_{1\theta}=\sqrt{2}\sigma_\theta$, so that the final relation is

$$\alpha_c=2.14\sqrt{2}\sigma_\theta. \tag{12}$$

Thus by measuring σ_θ, the characteristic half width of a channel peak, α_c can be determined. As a comparison it is worthwhile mentioning that if the peak profiles are perfect Gaussian distributions, one would obtain a factor $2\sqrt{2}$ relating α_c and σ_θ.

Figure 5(a), (b), and (c) show the critical angle for channeling α_c as a function of the average ion energy $\bar{E}$ in the foil for the three low-index crystallographic directions ⟨011⟩, ⟨001⟩, and ⟨112⟩. The average ion energy is obtained from the incident ion

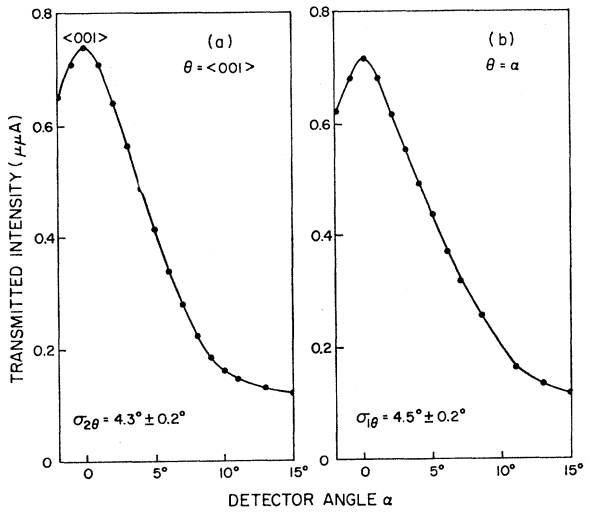

FIG. 3. (a) The transmitted intensity is shown as a function of the detector angle α with respect to the forward direction for the foil oriented on the ⟨001⟩ channel. The characteristic half width $\sigma_{2\theta}=\sigma_\alpha$ is found to be $\sigma_{2\theta}=4.3°\pm0.3°$. The same foil is used as in Fig. 2. (b) The transmitted intensity is shown as a function of α with the foil tilted so that $\theta=\alpha$ about the ⟨001⟩ channel. The characteristic half width is found to be $4.5°\pm0.3°$. The same foil is used as in Fig. 2.

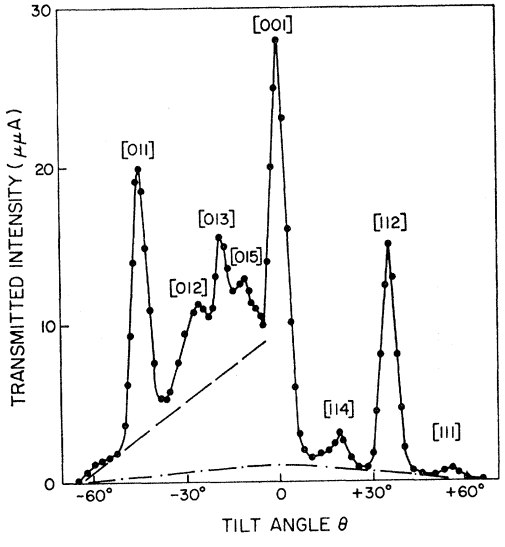

FIG. 4. The transmitted intensity is shown as a function of θ in the two planes (100) and (110) for 8.5 keV D^+ ions. The incident current is 1000 $\mu\mu$A. The dot-dashed line indicates the randomly scattered ions. The difference between the dashed line and the dot-dashed line represents the planar channeling in the (100) plane. No planar channeling is seen in the (110) plane. The widths of the stronger peaks are quite a bit smaller than in Fig. 2. The same foil is used as in Fig. 2.

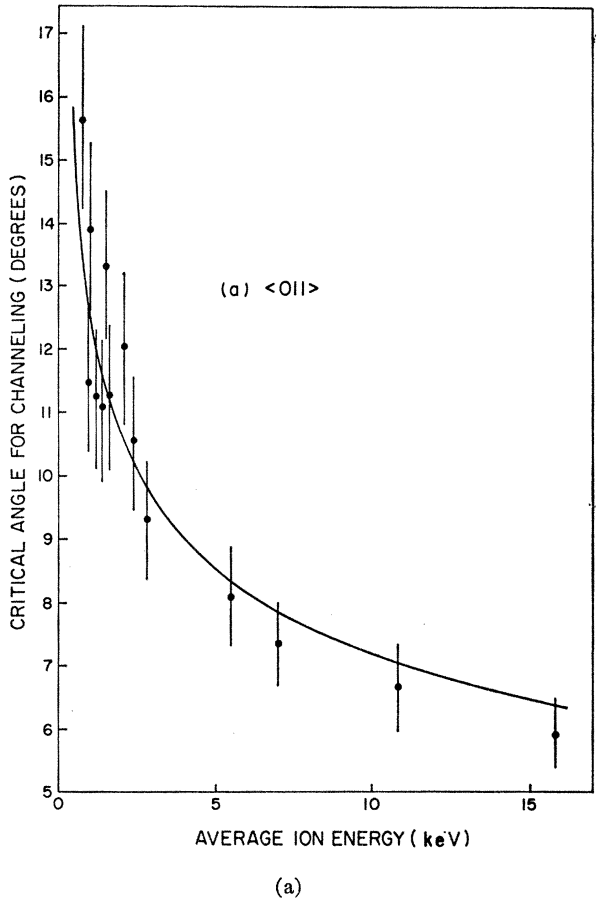

FIG. 5. The critical angle for channeling ψ_2 is shown as a function of the average energy $\bar{E}$ of the ions in the crystal for the three channels (a) $\langle 011 \rangle$, (b) $\langle 001 \rangle$, and (c) $\langle 112 \rangle$. The solid lines are the theoretical curves using the theory by Lindhard with a value of $C=2.15$. The filled circles represent the experimental critical angles α_c and the vertical bars show the errors. The errors in energy vary from 0.3 keV at 1 keV to 0.5 keV at 17 keV. Most of the spread of the experimental points is due to the fact that the information is obtained using several films with different thickness between 180 and 260 Å.

energy E by the relation $\bar{E}=E-\frac{1}{2}\Delta E_{\mathrm{mp}}$. The solid curves represent the theoretical expression $\psi_2(E)$ and the filled circles represent the experimental values. Several different foils have been used in order to avoid errors from contamination build up and radiation damage. The foil thickness cannot be exactly reproduced in the evaporation equipment. Consequently, the foil thicknesses are found to range between 180 and 260 Å. This spread in thickness explains most of the spread in α_c. It is seen in Fig. 5 that the approximate expression given by Lindhard fits the experimental points for all three of the channels if the constant C is given the value 2.15. The low-energy value ψ_2 is the appropriate one to use since it can be seen that $E'=810$ keV for an H^+ ion in the low-index directions.

The critical angle for channeling ψ_2 is symmetrically dependent on Z_1 and Z_2. The choice of practical values for Z_2 is limited but it is possible to get suitable silver foils for use as targets. Silver foils were used in a few of the experiments but the fact that ψ_2 varies as $[Z_1Z_2/(Z_1^{2/3}+Z_2^{2/3})]^{1/4}$ causes only a small change in

ψ_2 for a change of Z_2 from 79 to 49. The expected change of 5% is less than the experimental error.

The change in critical angle as a function of Z_1, is investigated by comparing the results for H^+, D^+, and He^+ ions. When H^+ ions are used instead of D^+ ions, the mass is decreased by a factor of 2, while Z_1 is constant. A comparison between D^+ ions and H^+ ions is made by using the same foil and the same incident energy E. A similar comparison is made between D^+ ions and He^+ ions. The use of these ions gives a change in both Z_1 and the mass M, of a factor of 2. The results of these measurements are best presented in Table II. An approximate correction is made for the different energy losses experienced by the three different particles, so that the critical angles are compared at about the same energy $\bar{E}$. Table II shows that there is no difference between $\sigma_\theta(H^+)$ and $\sigma_\theta(D^+)$. It is also seen that $\sigma_\theta(He^+)$ is larger than $\sigma_\theta(D^+)$ by a factor of 1.13 ± 0.04, which is significantly larger than 1. The theoretical factor expected from (8) is 1.17, so the experimental result agrees with the theoretical prediction.

CONCLUSION

The critical angles for channeling of light ions at low energies are in good agreement with the approximate expression for ψ_2 calculated by Lindhard if the arbitrary constant C in Lindhard's expression is assigned the value of 2.15.

ACKNOWLEDGMENTS

The authors would like to express their sincere gratitude to J. Lindhard, H. Shiött, and J. O. Anderson for helpful discussions and valuable comments.

PHYSICAL REVIEW VOLUME 159, NUMBER 2 10 JULY 1967

Proton Spin-Lattice Relaxation in $(Nd, La)_2Mg_3(NO_3)_{12}\cdot 24H_2O$ in High Fields and Low Temperatures*

T. E. GUNTER† AND C. D. JEFFRIES

Department of Physics, University of California, Berkeley, California

(Received 23 January 1967)

The dependence of the proton relaxation time $T_{1\rho}$ on field H and temperature T in a crystal of $(Nd, La)_2Mg_3(NO_3)_{12}\cdot 24H_2O$ grown from a solution containing 1% Nd is measured over the ranges $10 \leqq H \leqq 50$ kOe and $0.5 \leqq T \leqq 3$°K using a He^3 cryostat in a superconducting solenoid. Over these wide ranges the relaxation data for $c \perp \mathbf{H}$ are well fitted by the expression

$$T_{1\rho}^{-1} = 2.1\times10^{-16}H^3 \coth(2.7\beta H/2kT)\ \mathrm{sech}^2(2.7\beta H/2kT) + 9.9\times10^{-8}H \coth(4.4\beta H/2kT)\ \mathrm{sech}^2(4.4\beta H/2kT)\ \mathrm{sec}^{-1},$$

where β = Bohr magneton, k = Boltzmann's constant, and H is in Oe. The first term is due to Nd^{3+}, the second to a small impurity of a non-Kramers ion, possibly Fe^{2+}. Both are in agreement with predictions from a shell-of-influence model, including diffusion effects. At 19.5 kOe and 0.5°K, we find $T_{1\rho}=40$ h, showing that dynamically induced proton polarization in this crystal can be maintained for very long times. In particular, the data display well the sech^2 factor, leading to exponentially increasing proton relaxation times at high fields and low temperatures, $T_{1\rho}(T) \propto \exp(g\beta H/kT)$, due to the depopulation of the upper Nd^{3+} Zeeman level.

I. INTRODUCTION

In an earlier work,[1] referred to as S-J, dynamic proton polarization and relaxation were studied in crystals of diamagnetic lanthanum magnesium nitrate containing a small fraction of paramagnetic Nd^{3+} ions, denoted by Nd:LaMN. Large proton polarizations (70%) are obtained with this crystal, and it is now being used in many polarized proton targets.[2] The object of this paper is to extend the relaxation studies to higher fields ($H\approx50$ kOe) and lower temperatures ($T\approx0.5$°K) in order to test further the theory of nuclear relaxation as well as to provide data for possible operation of targets at these fields and temperatures. A brief discussion of dynamic polarization is included.

* Supported in part by the U.S. Atomic Energy Commission, Contract No. AT(11-1)-34, Project 20; Report No. UCB-34P20-130.

† National Science Foundation predoctoral Fellow. Present address: Donner Laboratory, Lawrence Radiation Laboratory, Berkeley, California.

[1] T. J. Schmugge and C. D. Jeffries, Phys. Rev. **138**, A1785 (1965); see also Phys. Rev. Letters **9**, 268 (1962).

[2] O. Chamberlain, C. D. Jeffries, C. H. Schultz, G. Shapiro, and L. Van Rossum, Phys. Letters **7**, 293 (1963); M. Borghini, M. Odehnal, P. Roubeau, C. Ryter, G. Coignet, L. Dick, and L. di Lella, in *Proceedings of the International Conference on High-Energy Physics, Dubna, 1964* (Atomizdat, Moscow, 1965). For a recent survey of targets, see *Proceedings of the International Conference on Polarized Targets and Ion Sources, Saclay, 1966* (La Documentation Francois, Paris, 1967).